

Supplement of Biogeosciences, 12, 769–779, 2015
<http://www.biogeosciences.net/12/769/2015/>
doi:10.5194/bg-12-769-2015-supplement
© Author(s) 2015. CC Attribution 3.0 License.



Supplement of

Characterization of incubation experiments and development of an enrichment culture capable of ammonium oxidation under iron-reducing conditions

S. Huang and P. R. Jaffé

Correspondence to: P. R. Jaffé (jaffe@princeton.edu)

Supplemental Information

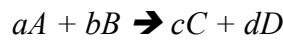
Huang and Jaffe

Characterization of incubation experiments and development of an enrichment culture capable of ammonium oxidation under iron reducing conditions

1. Supplemental Methods

1.1 Thermodynamic Consideration of Feammox

The change in Gibbs free energy of Equation 1 was calculated to determine the thermodynamic feasibility of the Feammox reactions using the following equation:



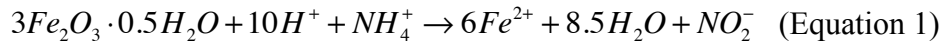
$$\Delta G_r = \Delta G_r^0 + RT \ln \frac{(C)^c (D)^d}{(A)^a (B)^b}$$

and:

$$\Delta G_r^0 = c\Delta G_{fC}^0 + d\Delta G_{fD}^0 - a\Delta G_{fA}^0 - b\Delta G_{fB}^0$$

R is the gas constant, which equals 0.008314 kJ mol⁻¹. K, and T is the absolute temperature in ° Kelvin (297.15 K). Free energies of formation were obtained from Stumm and Morgan (1996): $\Delta G_f^0(\text{NH}_4^+) = -79.37$ kJ mol⁻¹, $\Delta G_f^0(\text{NO}_2^-) = -37.2$ kJ mol⁻¹, $\Delta G_f^0(\text{H}_2\text{O}) = -237.18$ kJ mol⁻¹, $\Delta G_f^0(\text{Fe}^{2+}) = -78.87$ kJ mol⁻¹. $\Delta G_f^0(\text{Fe}_2\text{O}_3 \cdot 0.5\text{H}_2\text{O}) = -711$ kJ mol⁻¹ (Majzlan *et al.*, 2004). For biogeochemical reactions

involving H^+ , requires converting from standard condition (pH=0) to biochemical conditions: $\Delta G^{0'} = \Delta G^0 + m\Delta G_f'(H^+)$, where m is the net number of H^+ in the reaction and $\Delta G_f'(H^+)$ is calculated as $-5.69 \text{ kJ mol}^{-1}$ per pH unit (Madigan *et al.*, 2002). The chemical activity values used in the calculation are based on our incubation experiments: $C_{NH_4^+} = 2 \text{ mmol L}^{-1}$, $C_{NO_2^-} = 10 \mu\text{mol L}^{-1}$, $C_{Fe^{2+}} \leq 0.01 \mu\text{mol L}^{-1}$ (detection limit), respectively, and pH = 4.0. The dissolved Fe(II) was below the ferrozine method detection limit in the solution due to its sorption onto the Fe(III) oxides. Measurable dissolved Fe was only present in the samples extracted with 0.5M HCl. An activity of 1 was used for the solid-phase Fe(III) oxide minerals, and water.



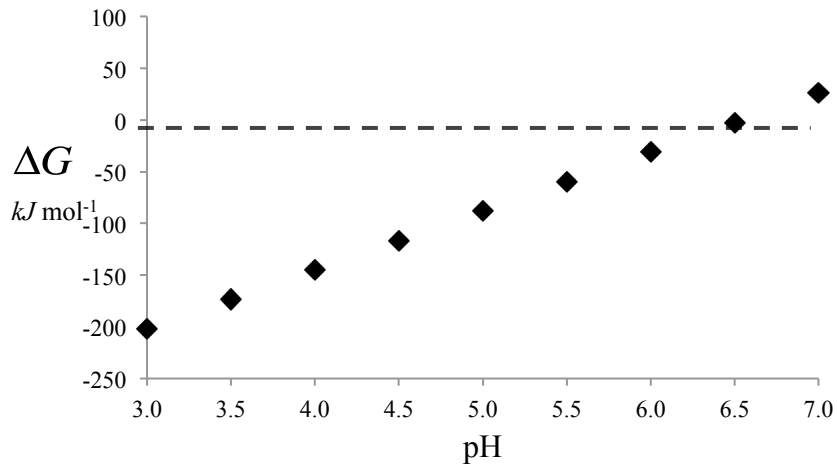
$$\Delta G_r \leq [6\Delta G_{fFe^{2+}}^0 + 8.5\Delta G_{fH_2O}^0 + 1\Delta G_{fNO_2^-}^0 - 3\Delta G_{fFe_2O_3 \cdot 0.5H_2O}^0 - 10\Delta G_{fH^+}^0 - 1\Delta G_{fNH_4^+}^0] \\ + (0.008314 \text{ kJ mol}^{-1})(297.15 \text{ K}) \ln \frac{(C_{Fe^{2+}})^6 (C_{H_2O})^{8.5} (C_{NO_2^-})^1}{(C_{Fe_2O_3 \cdot 0.5H_2O})^3 (C_{H^+})^{10} (C_{NH_4^+})^1}$$

$$\Delta G_r \leq [6(-78.87) + 8.5(-237.18) + 1(37.2) - 3(-711) - 10(4 \times -5.69) - 1(-79.37)] \\ + (0.008314 \text{ kJ mol}^{-1})(297.15 \text{ K}) \ln \frac{(10^{-8})^6 (1)^{8.5} (10^{-5})^1}{(1)^3 (10^{-4})^{10} (2 \times 10^{-3})^1}$$

$$\Delta G_r \leq -145.08 \text{ kJ mol}^{-1}$$

The \leq sign is because we used an upper limit (detection limit) for the Fe(II) concentration.

A graph of ΔG vs. pH shows that when maintaining all species concentrations constant except H^+ , Feammox should not be feasible when the pH is above 6.5. Hence, we should expect Feammox to occur in acidic environments.



Note: Ferrihydrite is unstable, and with a few exceptions (Majzlan *et al.*, 2004), not many values for its ΔG_f^0 have been reported. Hence, many authors use $\text{Fe}(\text{OH})_3$ as a stand in for ΔG_r calculations involving ferrihydrite. Using $\text{Fe}(\text{OH})_3$ will also result in a negative ΔG_r , when NH_4^+ is oxidized to NO_2^- and $\text{Fe}(\text{OH})_3$ reduced to $\text{Fe}(\text{II})$ (Yang *et al.*, 2012). The same is true for goethite as the $\text{Fe}(\text{III})$ source (Clement *et al.*, 2005).

1.2 PCR amplification, DGGE analysis and pyrosequencing

Bacterial universal 16S rRNA gene primer sets V3-2/ V3-3 (Jensen *et al.*, 1998) and 27f /519r (Lane, 1991) were used for PCR amplification. Each 25 μL reaction mixture contained 2.5 μL 10 \times PCR Buffer (500 mM KCl, 25 mM MgCl_2 , 200 mM Tris-HCl [pH 8.4], 0.1% Triton X-100), 2.0 μL 2.5mM dNTP mixture (Takara, Japan), 0.3 μL of 10 μM V3-2 and V3-3, 0.13 μL 5U Taq polymerase, 1 μL of template DNA, and 18.77 μL sterilized ddH₂O. The PCR protocol was as follows: 30 s initial denaturation at 94 °C; 10 cycles with each cycle consisting of 30 s of denaturation at 94 °C, 30 s of annealing at 61°C (the temperature of anneal decreased 0.5 °C after each cycle), and 40 s extension at 72 °C; 25 cycle with each cycle included 30 s denaturation at 94°C, 30 s annealing at 55 °C, and 40 s extension at 72 °C; followed by a final 5 min extension at 72 °C. PCR products stained with 0.02 $\mu\text{L mL}^{-1}$ Genefinder were visualized on 1% (w/v) agarose gel

at 120 V for 20 min, and visualized under SYNGENE Genesnap. A much higher degree of diversity was observed with primer sets V3-2/ V3-3, hence its DGGE products were used for the following analysis.

After the DGGE was performed, all visible bands were excised from the gel and used as templates for re-amplification, using primer set V3-1/V3-2 (Jensen *et al.*, 1998). The PCR program was initiated with 30 s at 94 °C, followed by 40 cycles of 5 s at 94 °C, 30 s at annealing at 56°C, and 30 s at 70 °C. The PCR products were purified using Qiaquick PCR preps (Qiagen, Valencia, CA) and cloned into a pGEM-T vector (Promega, USA). Positive recombinant clones were identified by PCR, and the PCR products were cleaned with ExoSap treatment and sequences were conducted by Genewiz, Inc., USA. Clone libraries from 12 samples resulted in 721 sequences of partial 16S rRNA gene fragments and the sequences were grouped into operational taxonomic units (OTUs) based on a 5% sequence distance cutoff calculated using the DOTUR program (Schloss and Handelsman, 2005). Six groups of bacteria were classified via a phylogenetic analysis using the Bayesian inference (BI) (Huelsenbeck *et al.*, 2001), implemented with MrBayes version 3.1.2 (Ronquist *et al.*, 2003). A best fit model of nucleotide substitution was identified using the Akaike information criterion (AIC) (Akaike, 1973) as implemented in MrModelTest 2.3 (Nylander, 2004). Bayesian analysis was carried out using GTR+I+G model selected by MrModelTest 2.3, in which model parameters were treated as unknown and estimated through the BI. The following settings were applied: implementing two Markov chain Monte Carlo (MCMC) runs, running four simultaneous Markov chains for 19 million generations, and sampling the Markov chains every 100 generations. Tracer V1.5 (Rambaut and Drummond, 2009) was used to judge convergence of the Bayesian Markov chain Monte Carlo runs. The first 10,000 sampled trees were discarded as burn-in. A consensus tree as show in Fig. 1 was constructed from the remaining sampled trees. Sequences reported in this study were deposited in GenBank database under accession numbers KC581755 -KC581779.

Approximately 2.5 ng of each DNA extract from samples collected from the incubation on days 0, 30, 90, 160 and from the membrane reactor after 150 days of reactor operation were used for 454 pyrosequencing analysis. To amplify a 16S rRNA gene fragment of the appropriate size and sequence variability for the 454 pyrosequencing, specific primers Bact-338F1(CCTACG GGRGGCAGCAG) /909R(CCGTCAATTYHTTTRAGT), targeting the V3-V5 region of the 16S rRNA gene of bacteria were chosen (Pinto and Raskin 2012). The PCR conditions used were 94°C for 2 min, 20 cycles of 94°C, 45 s denaturation; 55°C, 45 s annealing and 72°C, 1 min extension; followed by 72°C, 6 min. After 20 rounds of amplification, another 3 rounds of amplification were done to add the A and B adapters required for 454 pyrosequencing to specific ends of the amplified 16S rRNA fragment for library construction (Margulies *et al.*, 2005). Approximately 4 ng/µl of 16S rRNA gene fragment from each soil samples was required to construct the five libraries for 454 sequencing. Polymerase chain reaction products were cleaned using the QIAquick PCR Purification Kit (Qiagen) following the manufacturer's instructions, quantified using a Qubit Fluorometer (Invitrogen), and then sent for 454-pyrosequencing using a Roche/454 GS FLX sequencer

A total of 19,021 partial 16S rRNA sequences were obtained from the five soil samples. The sequences were then passed through the DOTUR program to further reduce errors as outlined previously (Schloss and Handelsman, 2005). Briefly, after trimming, pre-clustering, removal of chloroplast sequences and alignments, a total of 10172 sequences remained. These were clustered with the average neighbor algorithm with a 3% dissimilarity cutoff, which resulted in 1015 OTUs. (Pinto and Raskin 2012)

1.3 Primer design for real-time PCR assay

Two sets of primers, acd320f (5'-CGG TCC AGA CTC CTA CGG GA -3') - 432r (5'-GAC AGG GTT TTA CAG TCC GAA GA -3') and acm342f (5'- GCA ATG GGG

GAA ACC CTG AC-3') - 439r (5'-ACC GTC AAT TTC GTC CCT GC -3') were designed for *Acidobacteriaceae* bacteria A8 and *Acidimicrobiaceae* bacterium A6 respectively from clone libraries in this study, using an NCBI Primer-Blast program (<http://www.ncbi.nlm.nih.gov/tools/primer-blast>). This program did not show any putative sequences deposited in the GenBank, that amplified with the selected primers, could interfere with the experiment. The sequences of *Acidobacteriaceae* bacteria and *Acidimicrobiaceae* bacterium A6 acquired from this study did not exhibit any mismatches with the above primer sequences. Primers were then used for real-time PCR amplification in the soil samples from the incubation experiments.

1.4 Isotope tracer incubations

After 270 days of operation, Feammox enrichment slurries collected from the Feammox membrane reactor were used for isotope tracer incubations. Slurries were first incubated for 20 days in 50 mL vials under anaerobic conditions. Five treatments (n = 3 per treatment) were conducted as follows: (1) control treatment with only anoxic DI water; (2) $^{15}\text{NH}_4\text{Cl}$ addition; (3) $^{15}\text{NH}_4\text{Cl} + \text{Fe(III)}$; (4) $^{15}\text{NH}_4\text{Cl}$ and C_2H_2 addition; (5) $^{15}\text{NH}_4\text{Cl}$, C_2H_2 and Fe(III) addition. The final concentration of $^{15}\text{NH}_4\text{Cl}$ was 1 mmol L^{-1} , and 5 mmol L^{-1} of ferrihydrite was added as the Fe(III) source. 5 mL of pure C_2H_2 gas was added to the vials, which resulted in a final C_2H_2 concentration of $100 \text{ } \mu\text{mol L}^{-1}$. Samples were then incubated anaerobically for 7 days. The headspace gas was sampled every 24 hours for $^{15}\text{N}_2\text{O}$ analysis. All these processes were conducted in an anaerobic glove box. N_2O was determined by isotope ratio mass spectrometry (IRMS, Thermo Finnigan Delta V Advantage, Bremen, Germany). $^{15}\text{N}_2\text{O}$ concentration was also calculated as $^{15}\text{N}_2\text{O}$ atom% excess above its natural abundance, following methods described by Ding *et al.* (2014). $^{15}\text{N}_2\text{O}$ production rates were calculated from the linear change in $^{15}\text{N}_2\text{O}$ concentrations in the vial headspace between two given time points.

2. Supplemental Results

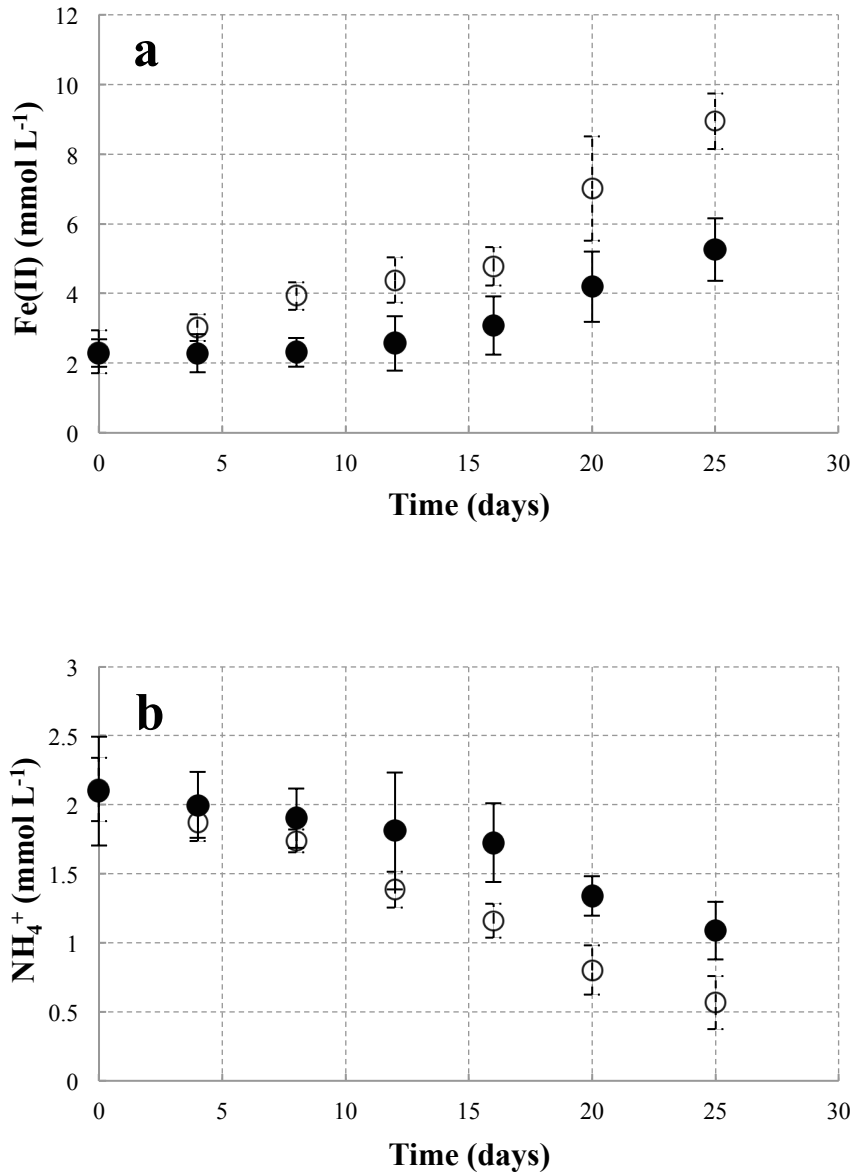


Figure S1. Concentration of Fe(II) and NH₄⁺ in 25-day incubation with NH₄Cl and ferrihydrite (○), NH₄Cl and goethite (●). The values represent the mean and standard error (n=3).

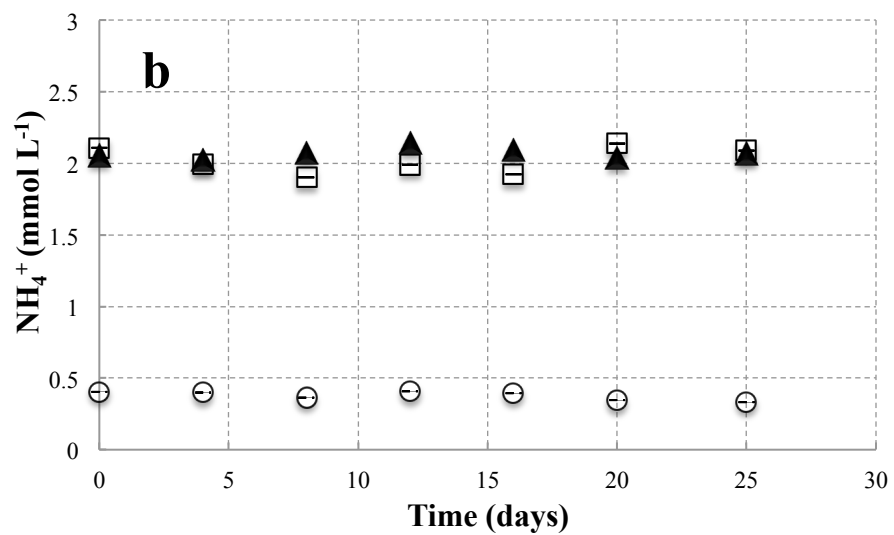
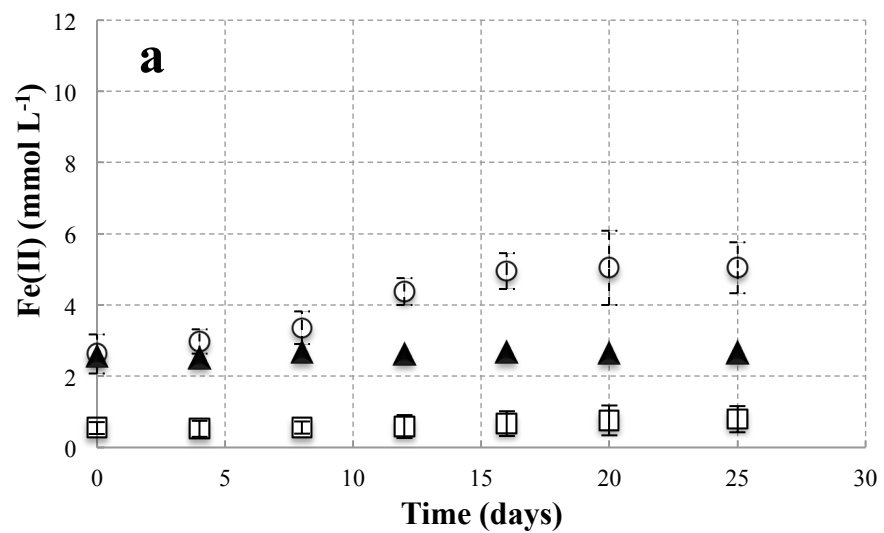


Figure S2. Concentration of Fe(II) and NH₄⁺ in 25-day incubations in samples with NH₄Cl (□), ferrihydrite (○), sterilized soil with NH₄Cl and ferrihydrite (▲). The values represent the mean and standard error (n=3).

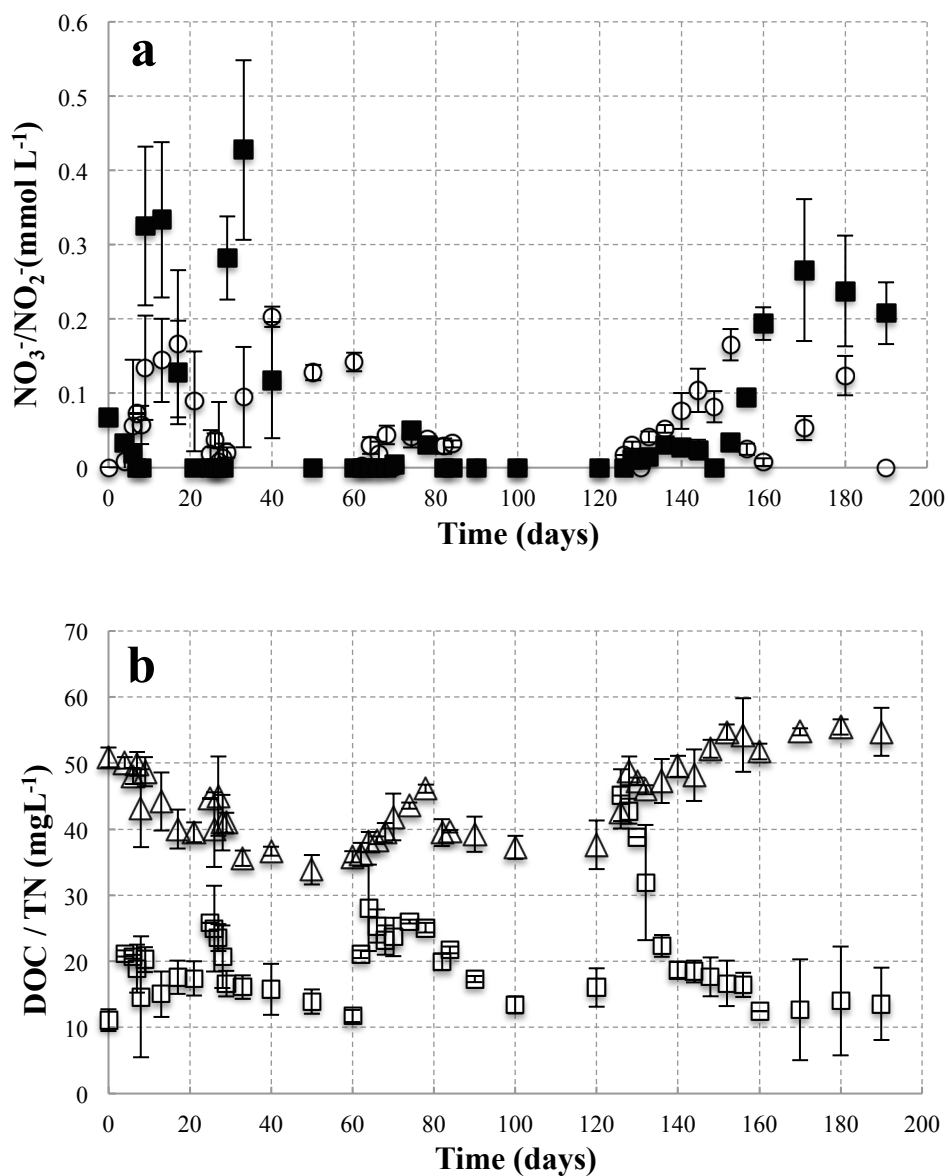
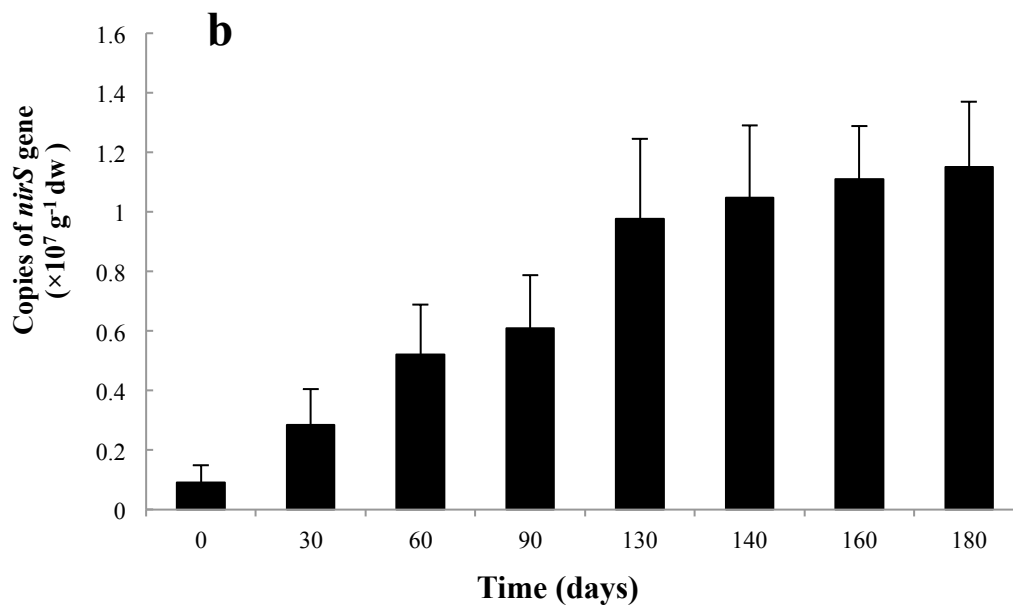
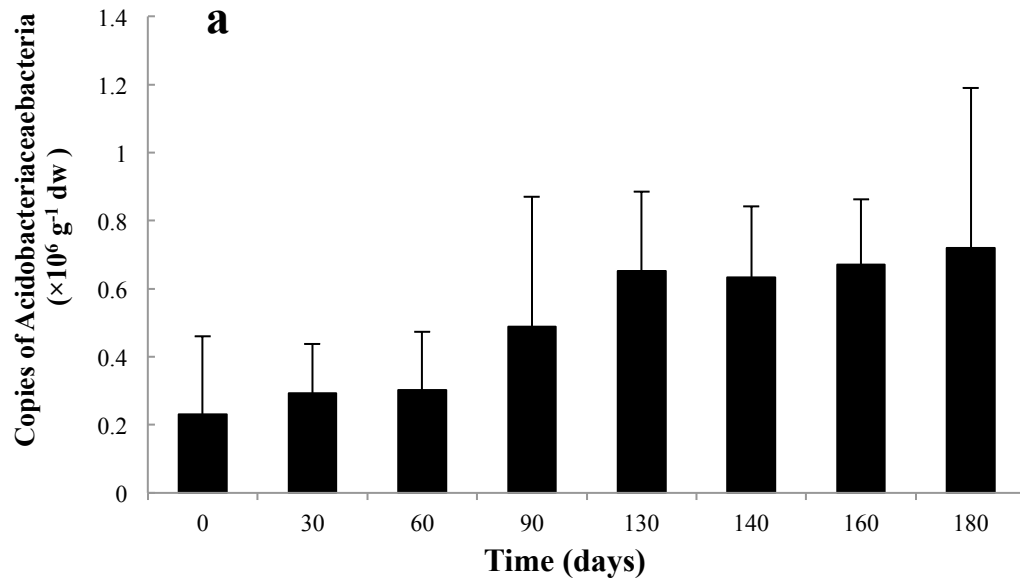
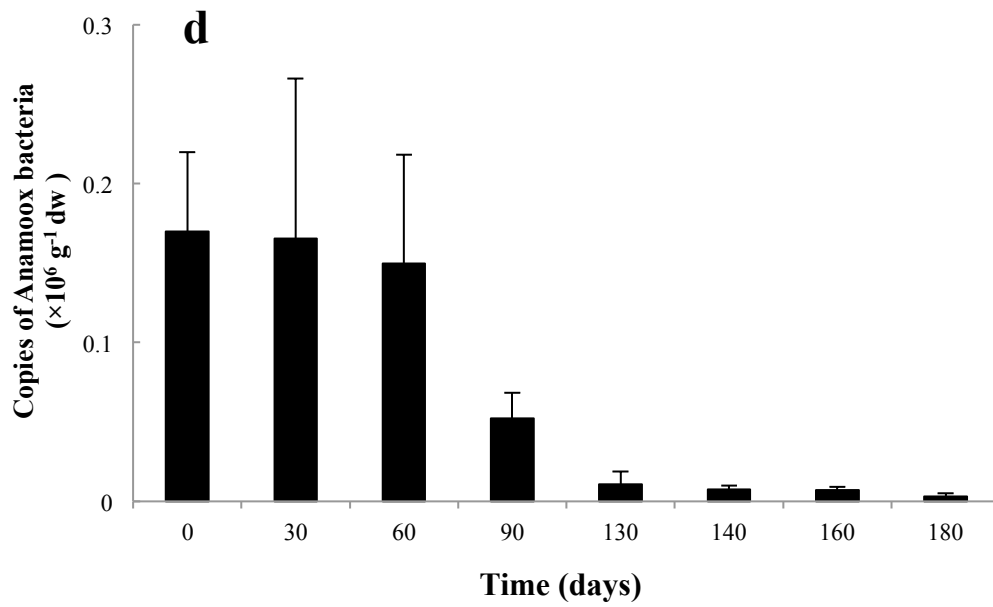
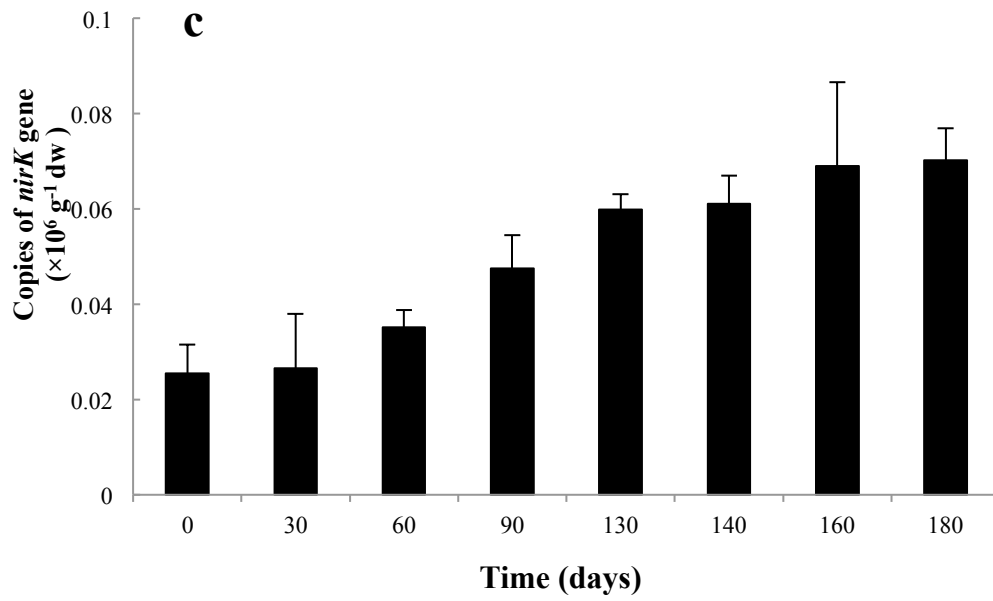


Figure S3. Concentration of (a) NO_3^- (\circ) and NO_2^- (\blacksquare) and (b) DOC (Δ) and TN (\square) during the 180 day incubation. $25 \text{ mmol L}^{-1} \text{ Fe(III)}$ was added on day 0. $1.0 \text{ mmol L}^{-1} \text{ NH}_4^+$ was added on days 4, 24, and 60. $0.2 \text{ mmol L}^{-1} \text{ NaHCO}_3$ was added on day 50 and day 90 of the incubation. $1.20 \text{ mmol L}^{-1} + 2 \text{ mmol L}^{-1}$ of NH_4Cl were added on day 125. The values represent the mean and standard error ($n=3$).





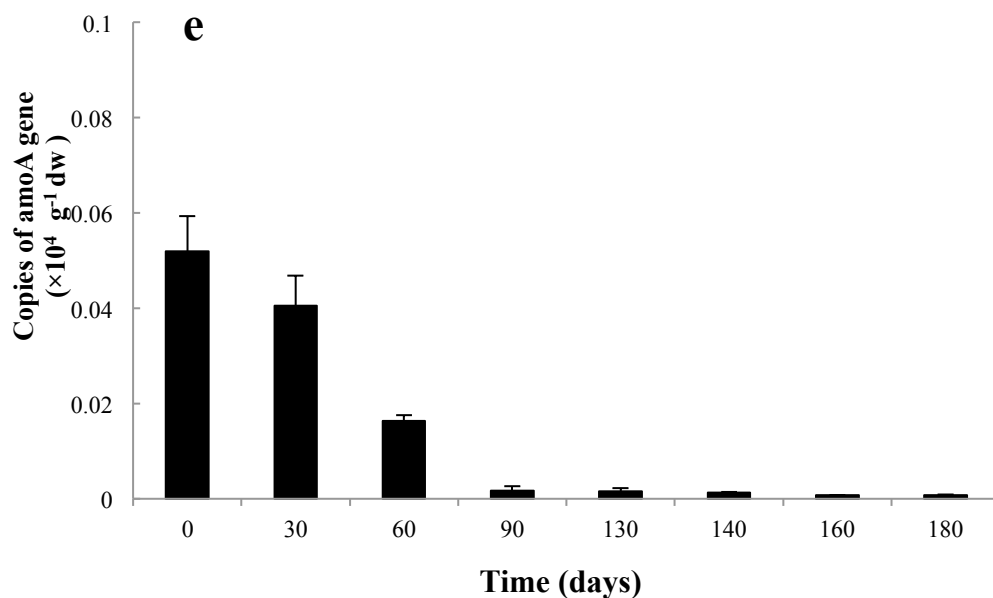
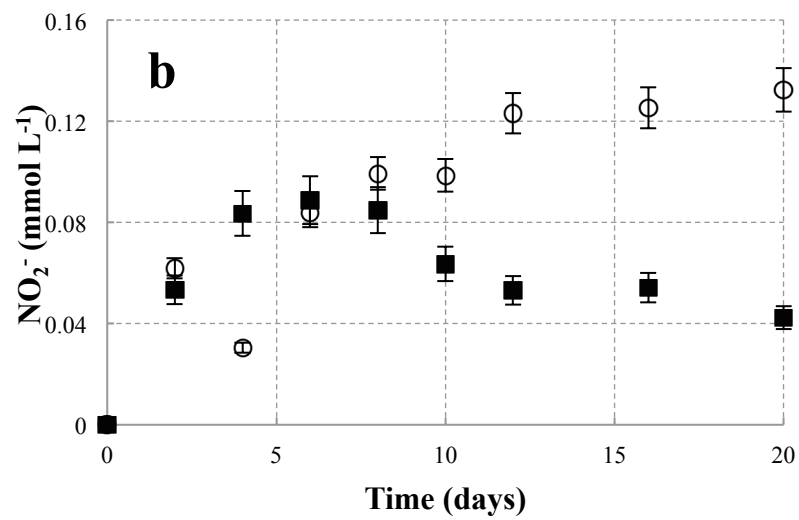
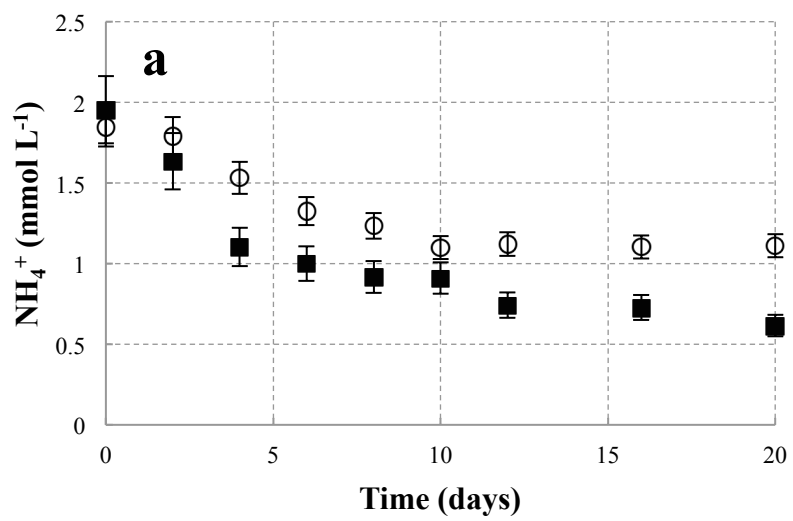


Figure S4. Copy numbers of (a) Acidobacteriaceae bacteria (DGGE band A8), (b) *nirS* gene, (c) *nirK* gene, (d) anammox bacteria and (e) *amoA* gene during 180 days of anaerobic incubation.



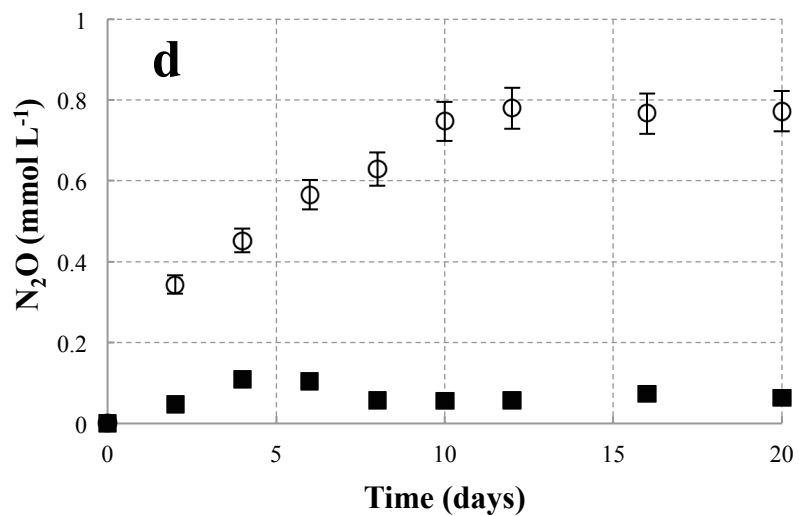
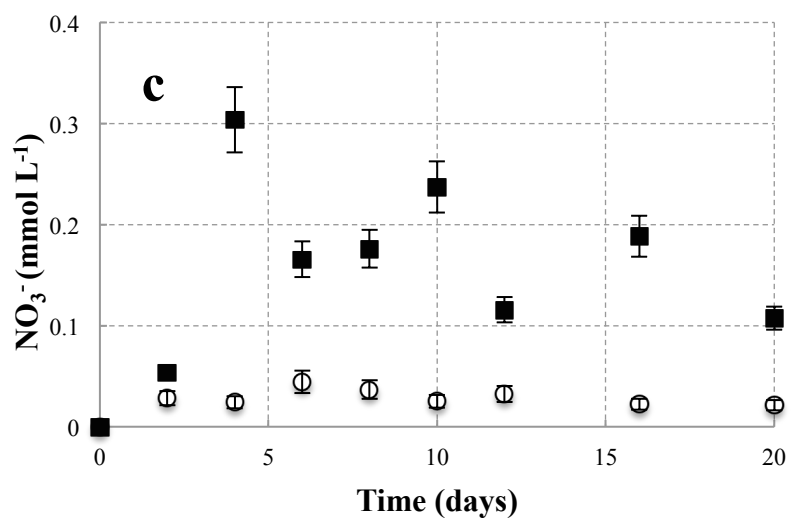


Figure S5. Concentration of NH₄⁺, NO₂⁻, NO₃⁻, and N₂O in the samples incubated with (○) or without (■) C₂H₂. The values represent the mean and standard error (n=3).

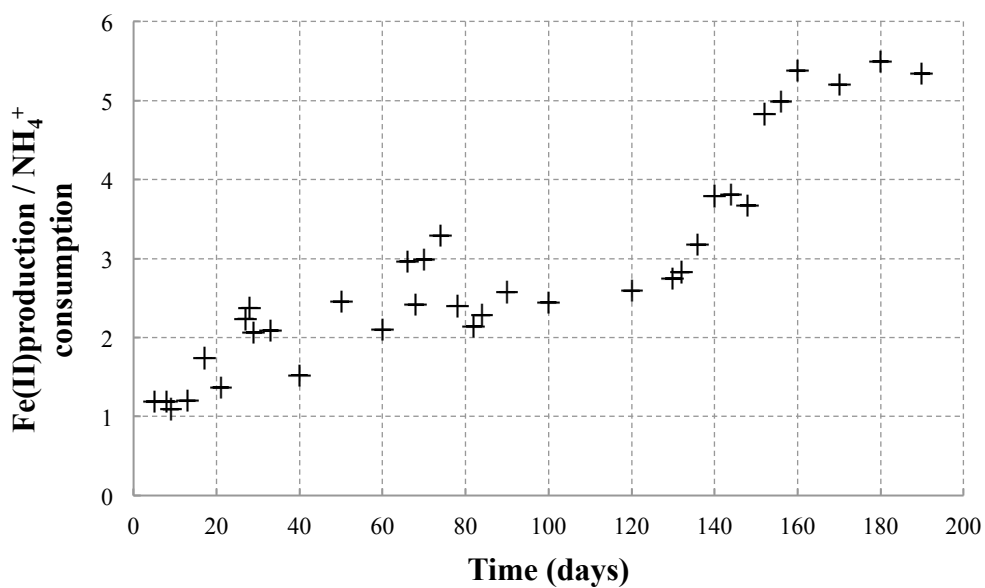


Figure S6 stoichiometry between the Fe(II) production and NH₄⁺ consumption during 180 day incubation. 25 mmol L⁻¹ Fe(III) was added on day 0. 1.0 mmol L⁻¹ NH₄⁺ was added on days 4, 24, and 60. 0.2 mmol L⁻¹ NaHCO₃ was added on day 50 and day 90 of the incubation. 1.20 mmol L⁻¹ + 2 mmol L⁻¹ of NH₄Cl were added on day 125. The values represent the mean ratio (n=3).

Table S1. Sequence analysis of bands excised from DGGE gels

Phylogenetic group	Band	Related sequence	Identity (%)
<i>Bacteroidetes</i>	A1	Uncultured Sphingobacteria bacterium clone ADK-BTh02-48 16S ribosomal RNA gene (EF520590)	93
		Flavobacterium sp. GNNN5_III 16S ribosomal RNA gene (JQ072049)	95
<i>Chloroflexi</i>	A3	Uncultured Bellilinea sp. clone 058 16S ribosomal RNA gene (GU556275)	99
		Ktedonobacter racemifer gene for 16S rRNA, partial sequence (AB510917)	93
	A12	Uncultured Chlorobi bacterium partial 16S rRNA gene, clone JML-1 (FN423885)	96
<i>Firmicutes</i>	A4	Eubacterium hadrum partial 16S rRNA gene, type strain DSM 3319T, clone 2 (FR749933)	99
	A11	Bacillus pocheonensis strain BJC15-D23 16S ribosomal RNA gene (JX483732)	100
	A10	Uncultured Paenibacillus sp. clone T1A4B 16S ribosomal RNA gene (HQ916801)	94
<i>Actinobacteria</i>	A6, B1, D6	Ferrimicrobium acidiphilum strain T23 16S ribosomal RNA gene (AF251436)	92
		Acidimicrobium ferrooxidans strain TH3 16S ribosomal RNA gene (EF621760)	90
	A6	Uncultured Ferrimicrobium sp. clone D.an-41 16S ribosomal RNA gene (JX505108)	95
	A13	Uncultured Actinobacteria Kmlps6-6 16S ribosomal RNA gene (AF289904)	98
<i>Acidobacteria</i>	B4	Uncultured Acidobacteria bacterium clone GYs1-54 16S ribosomal RNA gene (JX493091)	93
	A8, D11	Uncultured Acidobacteria bacterium clone 3OL11 16S ribosomal RNA gene(GQ342349)	97
		Geothrix sp. enrichment culture clone AP-FeEnrich1 16S ribosomal RNA gene (JX828409)	94

Proteobacteria

<i>Alphaproteobacteria</i>	B8	Uncultured <i>Sphingomonas</i> sp. clone B119 16S ribosomal RNA gene (HM452498)	100
<i>Deltaproteobacteria</i>	A5, C1,	Uncultured <i>Geobacter</i> sp. clone HZ-1d-7 16S ribosomal RNA gene (HQ875514)	99
	C2, B3	Uncultured <i>Cystobacteraceae</i> bacterium clone H3-27 16S ribosomal RNA gene, partial sequence (JF703480)	97
<i>Gammaproteobacteria</i>	A2	Uncultured <i>Pseudomonas</i> sp. isolate ODP1176A6H 26 B 16S ribosomal RNA gene (AY191355)	99
	A9	<i>Acinetobacter</i> sp. ACA7 16S ribosomal RNA gene (JN703731)	98
<i>BetaProteobacteria</i>	B2,B7	<i>Azoarcus denitrificans</i> Td-15 16S ribosomal RNA gene (L33688)	96
	B6	Uncultured <i>Ferribacterium</i> sp. Clone GS40to44-70 16S ribosomal RNA gene (JQ288478)	99
		Uncultured <i>Nitrospira</i> sp. isolate DGGE gel band 6 16S ribosomal RNA gene (JX901178)	96
	A7,B5, C3	Uncultured <i>Nitrosomonadaceae</i> bacterium clone PM5_-0.3-14 16S ribosomal RNA gene (JQ177857)	98
	A9,B9, C4, D14	Uncultured <i>Rhodocyclus</i> sp. clone W4S68 16S ribosomal RNA gene (AY691423)	97
	A9	<i>Comamonas</i> sp. 'ARUP UnID 223' 16S ribosomal RNA gene (JQ259419)	97

Table S2. Headspace ^{15}N - N_2O production rates for the incubations with $^{15}\text{NH}_4^+$.

	Control	$^{15}\text{NH}_4\text{Cl}$	$^{15}\text{NH}_4\text{Cl}+\text{Fe(III)}$	$^{15}\text{NH}_4\text{Cl}+\text{C}_2\text{H}_2$	$^{15}\text{NH}_4\text{Cl}+\text{C}_2\text{H}_2$ +Fe(III)
$^{15}\text{N}(\mu\text{g g}^{-1} \text{d}^{-1})$	<i>nd</i>	<i>nd</i>	0.072±0.023	<i>nd</i>	2.14±0.059

The values represent the mean and standard error (n = 3), *nd* = not detectable within a detection limit of 0.010 mg $^{15}\text{N} \mu\text{g g}^{-1} \text{d}^{-1}$.

3. Supplemental References

- Ding, L., An, X., Li, S., Zhang, G., Zhu, Y. 2014. Nitrogen Loss through Anaerobic Ammonium Oxidation Coupled to Iron Reduction from Paddy Soils in a Chronosequence. *Environ Sci Technol.* **48(18)**:10641-7.
- Lane, D. J. *16S/23S rRNA sequencing. In Nucleic acid techniques in bacterial systematics.* John Wiley and Sons Ltd. 1991.
- Majzlan, J.; Navrotsky, A.; Schwertmann, U. 2004. Thermodynamics of iron oxides: Part III. Enthalpies of formation and stability of ferrihydrite (Fe(OH)₃), schwertmannite (FeO(OH)_{3/4}(SO₄)_{1/8}, and ε-Fe₂O₃. *Geochim. Cosmochim. Acta.* 68, 1049–1059
- Madigan, M. T.; Martinko, J. M.; Parker, J. 2002. *Brock Biology of Microorganisms*, 10th ed. Appendix 1: energy calculations in microbial bioenergetics.
- Margulies, M., Egholm, M., Altman, W.E, Attiya, S., Bader, J.S., Bemben, L.A., Berka, J., Braverman, M.S, Chen, Y.J., Chen, Z. 2005. Genome sequencing in microfabricated high-density picolitre reactors *Nature*, 437, 376–380
- Ronquist, F. R.; Huelsenbeck, J. P. 2003. MrBayes 3: Bayesian phylogenetic inference under mixed models. *Bioinformatics.* 19, 1572–1574.
- Schloss, P. D.; Handelsman, J. 2005. Introducing DOTUR, a computer program for defining operational taxonomic units and estimating species richness. *Appl. Environ. Microbl.* 71, 1501–1506.
- Stumm, W.; Morgan, J. J. 1996. *Aquatic Chemistry: Chemical Equilibria and Rates in Natural Waters (John Wiley, New York)*